

TRANSIT TIME DERIVATION FOR HOT PLANET BOW-SHOCKS

P. Wilson Cauley,¹ Evgenya L. Shkolnik,¹ and Joe Llama²

¹*Arizona State University*

School of Earth and Space Exploration, Tempe, AZ 85287

²*Lowell Observatory*

Flagstaff, AZ 86001

(Received 2018/05/01; Accepted 2018/05/02)

Submitted to RNAAS

Keywords: methods: observational – planets and satellites: magnetic fields – planet-star interactions

Measurements of exoplanet magnetic fields remain elusive, although detections have now been confirmed in a small number of T-dwarfs (Route & Wolszczan 2012, 2013; Kao et al. 2016). While radio observations of auroral emission continue to be pursued, the possibility of indirectly measuring planetary magnetic fields via UV and optical observations of bow-shocks around hot planets remains a plausible path forward (Vidotto et al. 2010; Llama et al. 2011; Ben-Jaffel & Ballester 2013; Cauley et al. 2015). The upcoming Colorado Ultraviolet Transit Experiment (CUTE) aims, in part, to find such signals¹. Recent work has also suggested that estimates of hot Jupiter magnetic fields must be revised upward to take into account the extra heat being deposited into their interiors (Yadav & Thorngren 2017). If these field strength estimates are accurate, many known hot Jupiter systems should exhibit pre-transit interactions between the stellar wind and the planetary magnetosphere.

To aid in planning observations of signatures due to transiting bow-shocks, we derive an estimate of the contact time of the bow-shock nose with the stellar disk. This will allow telescope resources to be allocated more efficiently when searching for such signatures. The formula is a generalization of Eq. 19 from Vidotto et al. (2011b); the final form does not rely on a sky-projected value of r_m . We only consider leading shocks (see Vidotto et al. 2011a, for details). Our result is only approximate: if the density along the bow is sufficient, a portion of the bow away from the nose may cause a transit signal before the nose reaches the stellar disk. For reasonable bow geometries and densities, however, this should only amount to a difference of $\approx \pm 10$ minutes, which we consider negligible. A circular orbit is assumed since there is no closed-form for the distance along an arc of an ellipse. However, planets with $e \lesssim 0.1$, which encompasses the majority of transiting giant planets, should not show significant deviations from the derived pre-transit time for circular orbits.

Figure 1 shows the geometry of the transiting bow-shock. The planet is represented by the small black circle and the bow is shown as a parabola. The nose of the bow is at $s_m = (x_m, y_m)$ which is a distance r_m away from the center of the planet. The bow makes an angle θ_m with the tangent to the planet’s orbit. This angle is determined by the relative velocity of the planet and the stellar wind (see Vidotto et al. 2011a). The angle $\gamma = 90^\circ - \theta_m$ is marked in blue and the angle β , the angle between the star-planet line and star-bow nose line, in purple. The angle ϕ_{pl} , the planet’s angular distance from mid-transit, is shown in green. The distances a_{pl} and a_m represent the semi-major axis of the planet’s orbit and the bow nose orbit, respectively.

Corresponding author: P. Wilson Cauley
pwcauley@gmail.com

¹ <http://lasp.colorado.edu/home/cute/>

The bow nose transits when $x_m = -\sqrt{R_*^2 - b^2}$ where b is the planet's transit impact parameter in units of R_* ($b = 0$ in Figure 1). The position x_m is given by

$$x_m = -a_m \sin(\phi_{\text{pl}} - \beta) \quad (1)$$

which, for the transit condition to be met, is

$$-\sqrt{R_*^2 - b^2} = -a_m \sin(\phi_{\text{pl}} - \beta). \quad (2)$$

Using the law of cosines we can calculate a_m :

$$a_m = \sqrt{a_{\text{pl}}^2 + r_m^2 - 2a_{\text{pl}}r_m \cos \gamma} = \sqrt{a_{\text{pl}}^2 + r_m^2 - 2a_{\text{pl}}r_m \sin \theta_m} \quad (3)$$

where we have replaced $\cos \gamma$ with $\sin \theta_m$. We can also express β in terms of r_m , a_m , and θ_m :

$$\beta = \sin^{-1} \left(\frac{r_m}{a_m} \cos \theta_m \right). \quad (4)$$

The planet's angle from mid-transit ϕ_{pl} can be expressed as the distance along the arc subtended by ϕ_{pl} :

$$\phi_{\text{pl}} = \frac{v_{\text{orb}} \Delta t}{a_{\text{pl}}} \quad (5)$$

where v_{orb} is the planet's Keplerian orbital velocity and Δt is the time from mid-transit for the planet.

We can now combine Equation 2, Equation 4, and Equation 5 to solve for Δt as a function of the planet and bow parameters:

$$\Delta t = \frac{v_{\text{orb}}}{a_{\text{pl}}} \left[\sin^{-1} \left(\frac{\sqrt{R_*^2 - b^2}}{a_m} \right) + \sin^{-1} \left(\frac{r_m}{a_m} \cos \theta_m \right) \right] \quad (6)$$

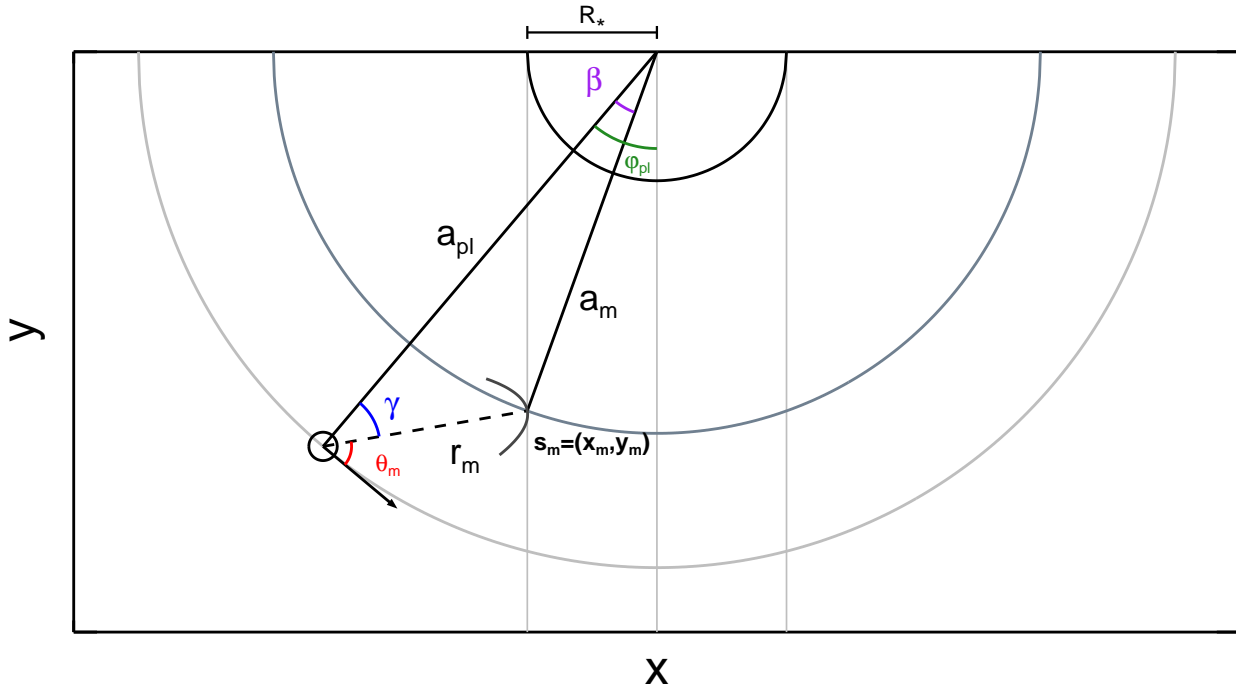


Figure 1. Bow-shock geometry.

where Δt is the beginning of the bow-shock transit relative to the transit midpoint of the planet. We have left Equation 6 in terms of a_m for clarity, although r_m is the more physically relevant parameter (see Eq. 9 of Llama et al. 2013). The value a_m can be calculated using Equation 3.

Equation 6 can be used to estimate the expected transit time of the bow-shock nose if approximations have been made for r_m and θ_m . This may allow, for example, a half-night of telescope time to be used to measure the bow-shock transit of a planet when Δt is small, rather than a full night.

Most transiting hot Jupiter hosts do not have measured magnetic fields (Fares et al. 2013; Mengel et al. 2017). This is important since the stellar field strength plays a large role in determining r_m . Similarly, the stellar wind speed at hot Jupiter orbital distances is poorly constrained for all stars. Thus Equation 6 should be used to consider the range of plausible bow-shock transit times given the range of reasonable values for the host star’s magnetic field and wind parameters. Finally, hot planets orbit through inhomogeneous regions of the stellar wind which may result in Δt changing as a function of time as the star’s activity level varies (Llama et al. 2013). This should be taken into account when considering values of Δt .

REFERENCES

- Ben-Jaffel, L., & Ballester, G. E. 2013, *A&A*, 553, A52
- Cauley, P. W., Redfield, S., Jensen, A. G., et al. 2015, *ApJ*, 810, 13
- Cauley, P. W., Redfield, S., Jensen, A. G., & Barman, T. 2016, *AJ*, 152, 20
- Fares, R., Moutou, C., Donati, J.-F., et al. 2013, *MNRAS*, 435, 1451
- Kao, M., Hallinan, G., Pineda, J. S., et al. 2016, *ApJ*, 818, 24
- Llama, J., Wood, K., Jardine, M. et al., 2011, *MNRAS*, 416, L41
- Llama, J., Vidotto, A. A., Jardine, M., et al. 2013, *MNRAS*, 436, 2179
- Mengel, M. W., Marsden, S. C., Carter, B. D., et al. 2017, *MNRAS*, 465, 2734
- Route, M., & Wolszczan, A. 2012, *ApJL*, 747, L22
- Route, M., & Wolszczan, A. 2013, *ApJ*, 773, 18
- Vidotto, A. A., Jardine, M., & Helling, Ch. 2010, *ApJ*, 722L, 168
- Vidotto, A. A., Jardine, M., & Helling, Ch. 2011, *MNRAS*, 411L, 46
- Vidotto, A. A., Jardine, M., & Helling, Ch. 2011, *MNRAS*, 414, 1573
- Yadav, R. K., & Thorngren, D. P. 2017, *ApJL*, 849, 12